Proceedings of the
Annual Stability Conference
Structural Stability Research Council
Baltimore, Maryland, April 10-13, 2018

Lateral–torsional buckling response of welded wide-flange girders

Xiao Lin Ji[1], Robert G. Driver[2], Ali Imanpour[3]

Abstract

Lateral–torsional buckling is a failure mode characterized by coupled lateral movement and twisting within an unbraced length of a steel member under flexure. The current Canadian steel design standard, CSA S16-14, prescribes unified design equations for predicting lateral–torsional buckling resistance that do not distinguish between rolled and welded sections. Results of recent numerical studies have shown that the current design equations to determine lateral–torsional buckling resistance may be unconservative for welded wide-flange steel girders. This is attributed to their welded nature, which produces residual stress distributions very different from rolled sections and may reduce their lateral–torsional buckling resistance. Furthermore, the design equations were developed based on studies using welding and fabrication methods that differ significantly from today's practices. Given the extensive use of wide-flange steel girders in building structures and bridges, there is an urgent need for better understanding and improvement of lateral–torsional buckling provisions in North American design standards. In this paper, S16's adequacy is examined by means of physical testing, with the aim of obtaining critical inelastic buckling moments. Test frames that allow out-of-plane movement (while maintaining continuous vertical load application) are implemented. Eleven large-scale specimens with laterally and torsionally pinned end conditions are tested to examine the effects of the cross-section geometry, residual stress distribution, and fabrication and welding procedures on the inelastic buckling resistance of welded wide-flange steel girders. The results of pre-test analyses aid in the design of test girders that are most affected by lateral–torsional buckling.

1. Introduction

1.1 Background

Lateral–torsional buckling (LTB) is a potential failure mode exhibited by unbraced beams and girders. When subjected to flexure, these members have much higher stiffness about the plane of loading (major principal axis) than about the plane of the minor principal axis. If there is insufficient lateral bracing, members may not reach their full cross-sectional capacity before LTB occurs. At the onset of LTB failure, flexural in-plane deformations change to simultaneous lateral movement and twisting, as shown in Fig. 1. During this time, load capacity remains constant at

[1] Master of Science Candidate, University of Alberta, <xlji@ualberta.ca >
[2] Professor, University of Alberta, <rdriver@ualberta.ca>
[3] Assistant Professor, University of Alberta, <imanpour@ualberta.ca>

first but decreases quickly as large deformation and yielding of the member occur (Galambos 1998), at which point the member's structural usefulness is terminated.

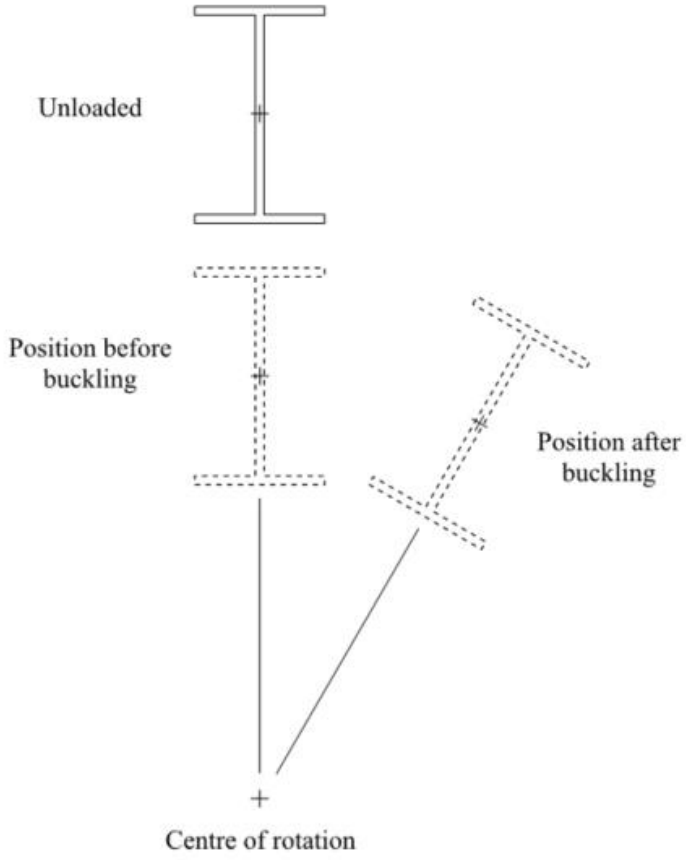

Figure 1: Lateral–torsional buckling (cross-section at mid-span)

As LTB is a limit state of unbraced members, it follows that unbraced length has a large influence on strength (critical moment), as shown in Fig. 2. Three ranges of behaviour can be observed: (1) elastic buckling, (2) inelastic buckling, and (3) cross-sectional capacity. In Canada, LTB resistance is determined in accordance with steel design standard CSA S16 (CSA 2014). It defines a strength curve using three individual, but related, design equations, a procedure that was first adopted into S16 in 1974 (MacPhedran and Grondin 2011). The base equations have since remained the same, with only slight modifications to the moment gradient factor. The provisions for doubly symmetric class 1 and 2 sections are shown in Eqs. 1-4.

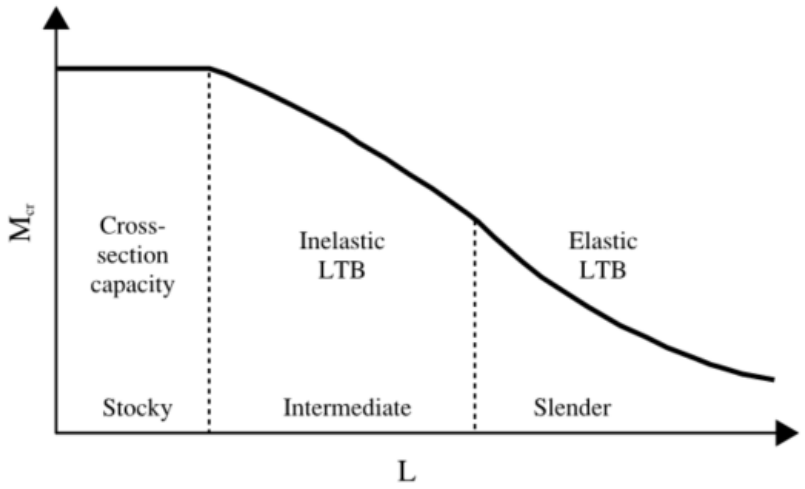

Figure 2: Variation of lateral–torsional buckling strength and behaviour with length

$$If\ M_u > 0.67M_p: \quad M_r = 1.15\phi M_p\left[1 - \frac{0.28M_p}{M_u}\right] \le \phi M_p \tag{1}$$

$$If\ M_u \le 0.67M_p: \quad M_r = \phi M_u \tag{2}$$

$$M_u = \frac{\omega_2 \pi}{L}\sqrt{EI_yGJ + \left(\frac{\pi E}{L}\right)^2 I_y C_w} \tag{3}$$

$$\omega_2 = \frac{4M_{max}}{\sqrt{M_{max}^2 + 4M_a^2 + 7M_b^2 + 4M_c^2}} \le 2.5 \tag{4}$$

where M_r is the factored moment resistance, ϕ is the resistance factor, M_p is the plastic moment capacity of the section, M_u is the critical elastic moment of the unbraced segment, ω_2 is the moment gradient coefficient, L is the length of the unbraced segment, E is the modulus of elasticity, I_y is the moment of inertia about the minor principal axis, G is the shear modulus of elasticity, J is the St. Venant torsional constant, C_w is the warping torsional constant, M_{max} is the maximum factored moment in the unbraced segment, and M_a, M_b, M_c are the factored moments at one-quarter point, midpoint, and three-quarter point of the unbraced segment, respectively.

1.2 Need for research

Currently, S16 uses unified equations that do not distinguish between rolled and welded sections. However, research has shown that these sections have significantly different residual stress distributions, which can be an important distinction during inelastic buckling. The design curve for the inelastic region (Eq. 1) was also developed based on experimental data of rolled sections (Galambos 1998). While the relative constancy of the design equations over time may speak to

their satisfactory performance, it also indicates a need to reassess the basis on which they were developed. Residual stresses are largely affected by welding and fabrication processes, which have changed significantly since the equations were first developed. The experimental data may no longer be representative of modern girders, leading to a lack of understanding of LTB resistance of welded wide-flange girders today. Therefore, there is an urgent need for a comprehensive reassessment of LTB provisions in North American design standards.

This paper presents the influential parameters on LTB resistance of welded steel girders and considers them in the development of the test matrix. A review of previous research studies is first presented. The LTB test program is then discussed; a testing method is proposed and the criterion used for test girder design and selection is defined.

2. Previous research

Studies of LTB began in the mid-1900s; closed-form solutions for strength were first developed for simple cases of elastic buckling (Timoshenko and Gere 1961). Numerical analyses have since followed to further the applicability to different moment distributions, end restraints, and monosymmetry. However, in design, the characterization of inelastic LTB has been largely empirical due to the varying extents of yielding (Galambos 1998). One of the first LTB tests was conducted by Dibley (1969), who tested 30 rolled I-sections of grade 55 steel under uniform moments. Further experiments on rolled sections were performed by Dux and Kitipornchai (1981) and Wong-Chung and Kitipornchai (1987) that studied effects of moment gradient and lateral bracing options on inelastic LTB capacity, respectively. Fukumoto (1976) conducted tests on 36 annealed and welded beams and girders; he concluded that the presence of residual stresses reduce the LTB strength of welded sections. Further research by Fukumoto and Itoh (1981) found residual stresses in welded sections to be significantly larger than those in rolled beams. Moreover, welded sections had lower ultimate moment capacities than rolled sections of similar geometry. A review of existing LTB experiments by Fukumoto and Kubo (1977) was performed to gather strength data of 156 rolled and 116 welded beams. However, it also revealed that the majority of LTB tests are either done on small-scale specimens (< 300 mm deep) or shorter unbraced lengths (< 5 m). Later, a statistical analysis on the strength variation of 25 rolled (Fukumoto et al. 1980) and 34 welded beams (Fukumoto and Itoh 1981), indicated that the variable value of the actual plastic moment has a large effect on LTB capacity. The large compressive residual stresses, particularly in welded sections, and initial crookedness are believed to be the potential cause of the variation in ultimate strength. As the section becomes more slender, the correlation between M_p and ultimate strength decreases. This conclusion is echoed in MacPhedran and Grondin's (2001) evaluation of S16 provisions. Using welded test data from Greiner and Kaim (2001), their comparison with S16 showed a large scatter of results focused primarily in the inelastic LTB and plastic capacity ranges. However, it was in particular the capacity of the inelastic LTB range that was over-predicted by S16. A numerical study by Kabir and Bhowmick (2016) reaffirms MacPhedran and Grondin's findings. They showed that S16 is somewhat unconservative for welded wide-flange girders in the inelastic LTB range; the difference between S16 and the numerical model becomes small for slender beams failing in elastic LTB. Other researchers have also observed similar trends of numerical simulations predicting capacities lower than experimental test results (Kim 2010; Greiner et al. 2001). A potential reason for the disconnect is assuming overly conservative initial imperfections and residual stress distributions in the numerical models (Subramanian and White 2017). While numerical simulations have suggested a need to reassess the current provisions for

inelastic LTB of welded sections, there is a lack of recent test data to corroborate the models. The existing database does not necessarily reflect modern girders and their updated welding and manufacturing processes, which greatly influences residual stresses.

3. Testing method

In response to the lack of up-to-date experimental data in the study of LTB, an experimental test program has been developed at the University of Alberta to examine the adequacy of the current S16 provisions. Eleven tests of large-scale welded wide-flange girders are proposed, with the aim of determining critical LTB moments in the inelastic range. Experimental moments can then be compared to the resistances predicted by S16 to evaluate the adequacy of the current provisions. The scope is focused on the inelastic LTB range as it has been an identified area of concern and there exist few experimental tests in this region (Fukumoto et al. 1971). Detailed residual stress measurements of all test girders will be recorded using sectioning and non-destructive ultrasonic testing in a companion project.

3.1 Test configuration

The proposed test uses flexurally simply supported and torsionally pinned boundary conditions. Girders will span 9.75 m (32 ft) and eight equally-spaced concentrated loads will be applied along the girder, as shown in Fig. 3. The only lateral supports provided to the girder are at its ends, allowing it to buckle out-of-plane along its entire span. A longer unbraced length also requires deeper specimens to be tested in order to fall within the inelastic LTB range, which is important as welded wide-flange girders are often used in large-scale applications. Additionally, as load points are unbraced, the uncertain effect of a continuous girder over lateral supports does not have to be accounted for in the unbraced length (Baker and Kennedy 1984). The loading configuration gives a moment distribution factor of $\omega_2 = 1.13$, which is calculated in accordance with Eq. 4.

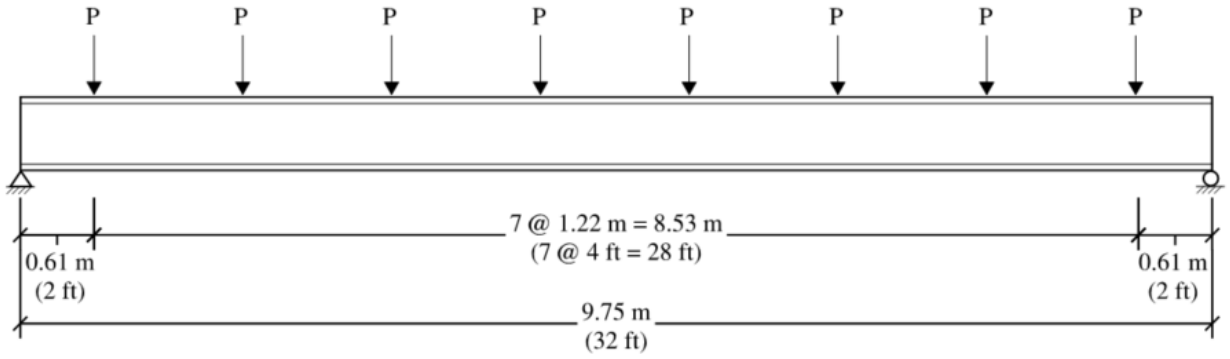

Figure 3: Loading configuration

3.2 Loading mechanism

A major challenge of conducting physical LTB tests is allowing for lateral movement while maintaining vertical load application. This requires the loading mechanism to move freely with the girder as it buckles out-of-plane, which is difficult to achieve. Though other researchers have compromised by laterally bracing the beam at the load points, this creates the disadvantage of shorter unbraced lengths. The proposed solution is the use of gravity load simulators, a loading apparatus developed for specimens permitted to sway (Yarimci et al. 1966). It is a pin-joined mechanism capable of swaying laterally while keeping load application close to vertical, as shown

in Fig. 4. No manual adjustments are required and the apparatus is free to sway from the equilibrium position in either direction.

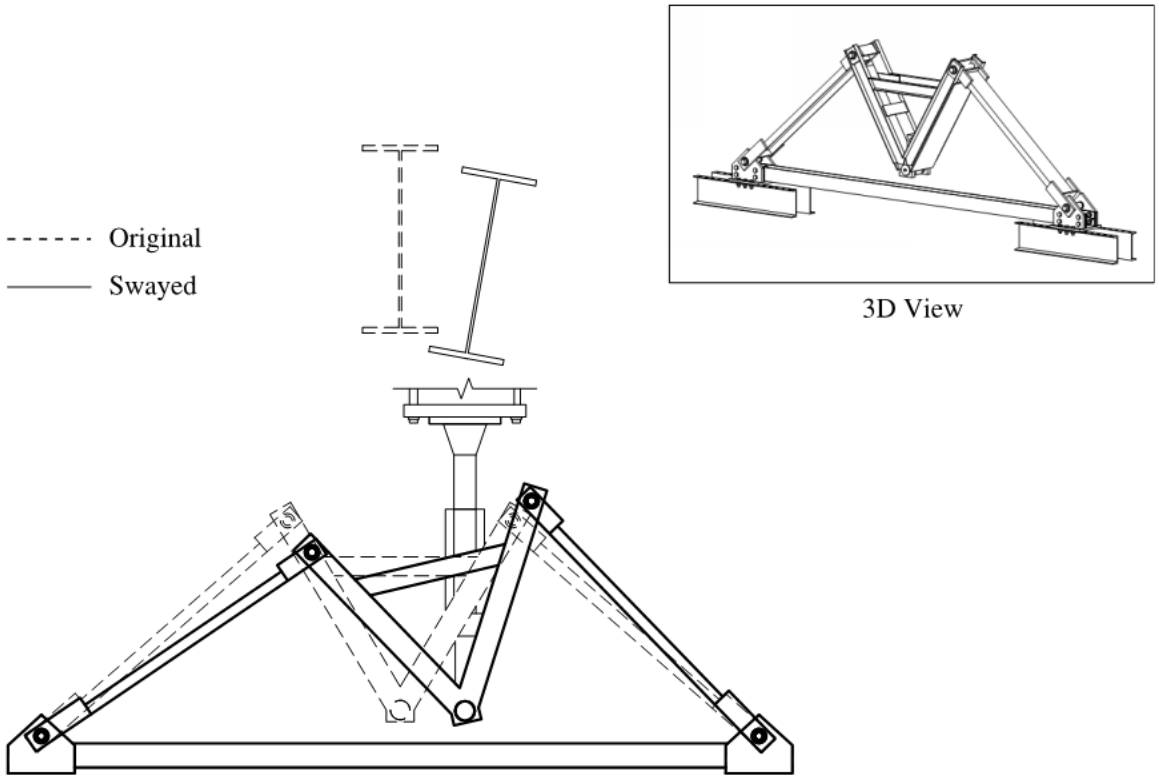

Figure 4: Gravity load simulator

By using gravity load simulators to apply concentrated loads at each of the eight load points, it is possible to achieve a 9.75 m unbraced length. Hydraulic actuators with a pull capacity of 385 kN will be attached to the gravity load simulators; as they are hydraulically dependent, the eight actuators have identical bore and piston diameters. The hydraulic actuators then connect to a collar, which wraps around the test girder. As the gravity load simulator pulls down, load is applied through the collar to the top flange of the girder, as shown in schematic diagrams of the test set-up in Figs. 5 and 6. Using CSI SAP2000 (CSI 2015), a static analysis was conducted to determine the capacity of the gravity load simulators in its equilibrium and swayed configurations. Allowing for the fact that the apparatuses must remain elastic during the test, the capacity was determined to be 380 kN. Hand calculations using beam-column design equations from S16 were completed to confirm the capacity. However, as Driver et al. (1997) successfully loaded the same gravity load simulators to 360 kN, it was decided that 360 kN would be the maximum load used for the proposed tests to provide an additional margin of safety.

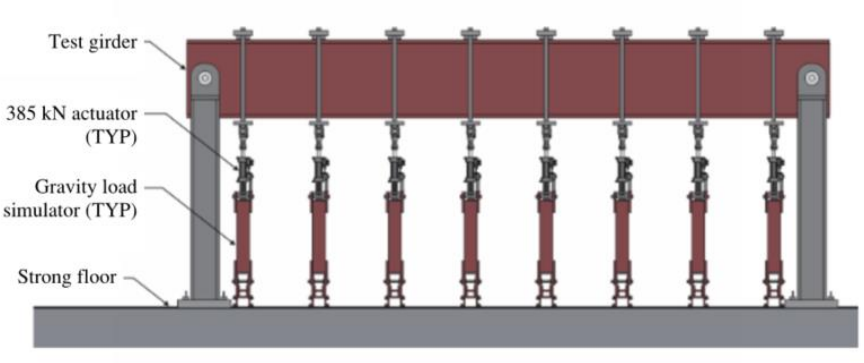

Figure 5: Elevation view of test set-up (schematic)

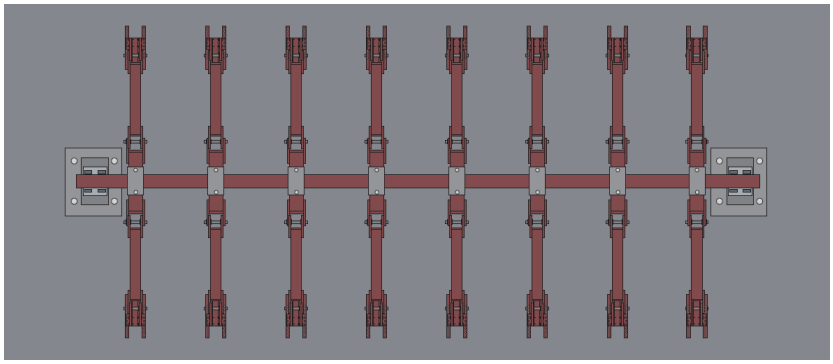

Figure 6: Plan view of test set-up (schematic)

4. Test matrix

In determining the test matrix, the overarching goal is to design girders so that the influence of LTB can be most observed—i.e., most sensitive to LTB. The study is focused in the inelastic buckling region. Three main influential factors are identified: cross-section geometry, residual stress distribution, and initial imperfections. It is accepted that initial local and global geometric imperfections will be present in the test girders (within the allowable limits specified in the S16 standard) and documented accordingly. However, for the matrix development the focus lies on cross-section geometry and residual stress distribution.

4.1 Cross-section geometry

Cross-section geometry involves flange width (b), flange thickness (t), web thickness (w), and section depth (d). To determine the dimensions most critical to LTB, a sensitivity analysis using MATLAB (Mathworks 2017) was performed. A series of surface plots were generated using x-axis as one cross-section dimension, y-axis as another, different cross-section dimension, and z-axis as LTB resistance. Surface plots allow the effect of one cross-section dimension on LTB to be observed relative to that of another, as shown in the surface plot of b vs. t in Fig. 7. In a given surface plot, the more critical dimension can be identified by assessing the slopes of the x-z and y-z planes. For example, from Fig. 7, it can be ascertained that flange width is more influential than flange thickness.

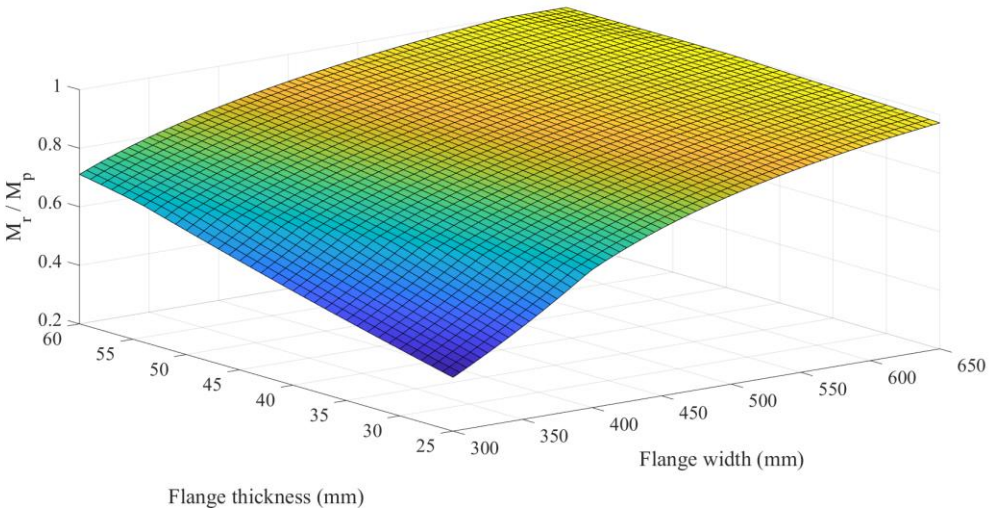

Figure 7: Surface plot of flange thickness vs. flange width vs. LTB resistance

To determine the extents of the *x*- and *y*-axes—i.e., the range to be used for each cross-section dimension—a list of standard welded wide-flange shapes that would fail in inelastic LTB under the proposed moment distribution was created. The smallest and largest possible value of each cross-section dimension was identified and this formed the range for the surface plot. In other words, the smallest and largest flange widths of standard welded wide-flange sections to fail in inelastic LTB are 300 mm and 650 mm, respectively (Fig. 7). In the surface plots, local buckling is not considered and all sections are assumed to be at least class 2. This is deemed acceptable for the current stage, as the purpose is to observe overall trends in each cross-section dimension's effect on LTB.

Through creating surface plots of various combinations of cross-section dimensions, a ranking of the most sensitive dimensions can be determined. The following combinations were used for the surface plots:

- *b* vs. *t*
- *b* vs. *d*
- *d* vs. *t*
- *d* vs. *w*
- *w* vs. *t*

The sensitivity analysis revealed that flange width and thickness are the dimensions most critical to LTB. This is consistent with expectations, as LTB is partly influenced by weak-axis flexural stiffness and the flanges of an I-shaped section are the most pertinent components.

4.2 Test girder design

In designing the test girders, there are several constraints that must be met. In addition to inelastic LTB, local buckling requirements must be satisfied, shear checks must pass, and the capacity of the gravity load simulators cannot be exceeded. A MATLAB code was written to implement these

constraints and generate the available cross-section geometries for at least class 2 and class 3 sections. The ranges of cross-section dimensions considered, with input from industry partners, are:

- b = 200 to 600 mm, in 10 mm increments
- t = {19.05, 22.225, 25.4, 31.75, 38.1}mm or {0.75, 0.875, 1, 1.25, 1.5}in
- w = {9.525, 12.7}mm or {0.375, 0.5}in
- d = 600 to 1000 mm, in 100 mm increments

After applying the constraints, the 4,000 possible cross-sections are reduced to 143 (3.6% of the original sample size). The available cross-sections are most limited by the shear check and gravity load simulator capacity. For class 3 sections, web slenderness is also dominant as it is difficult to achieve a sufficiently slender web that also has adequate shear strength but does not exceed the capacity of the gravity load simulators.

4.3 Residual stress

As residual stress is identified as an influential factor in LTB resistance, the aim is to choose sections most sensitive to different potential residual stress distributions. While detailed residual stress measurements will be taken on all test girders, a stress-based analysis is conducted to anticipate the effect of residual stresses, which can be used as part of test girder selection. The premise of the stress-based study is to begin analyzing LTB at the cross-section level by applying an increasing stress until the section has fully yielded. The yielding pattern takes into account a defined residual stress distribution, which is reflected by decreasing the moment of inertia accordingly. From the cross-section stresses the moment capacity of the section is calculated, which is then used to solve for the unbraced length in the elastic LTB equation, with the simplification of setting the St. Venant torsion term to zero (Eq. 5). Using the back-calculated unbraced length, a 'modified S16' predicted LTB capacity can be calculated. Original section properties (i.e., no yielding) are used and 'modified S16' refers to the simplification of M_u with St. Venant torsion again being zero (Eq. 6). By repeating this process for every increasing increment of applied stress, an LTB strength curve is created.

$$L = \left(\frac{\omega_2^2 \pi^4 E^2}{M_u^2} I_y C_w \right)^{1/4} \tag{5}$$

$$M_u = \frac{\omega_2 \pi^2 E}{L^2} \sqrt{I_y C_w} \tag{6}$$

Through the stress-based analysis, it is possible to determine the average percent difference between the modified S16 and the stress-based curve in the inelastic region. The purpose is to reveal trends in the effect of residual stress; the larger the percent difference, the greater the effect of residual stress on the cross-section, and the higher the potential effect on LTB. To begin the selection process, the percent difference is computed for each of the 143 available sections. The sections are first sorted into groups of the same section depth and web thickness. Within these groups, sections of similar slenderness (L/r_y within ±1 of each other) are compared by their percent

differences. Within a common slenderness ratio, the section with the largest percent difference is considered to be the most critical and remains as a potential test girder, while the other(s) is/are removed from consideration. The significance of conducting this process for sections with similar slenderness is to ensure geometrically comparable sections are evaluated against one another.

By carrying on this process, 143 sections were narrowed down to 109. The residual stress analysis also revealed an interesting trend. For girders of comparable slenderness, it was typically the member with the lowest inherent LTB capacity (as calculated by S16) that was most critical. This is congruous because the lower the inherent LTB capacity, the more the section's yielding pattern will be affected by varying residual stress distributions. Conversely, a higher inherent LTB capacity means the section is closer to reaching its full cross-sectional capacity and thus its inelastic patterns are not as sensitive. This trend is evident in Fig. 8, which shows sections of d = 600 mm and w = 12.7 mm before and after the residual stress sensitivity elimination.

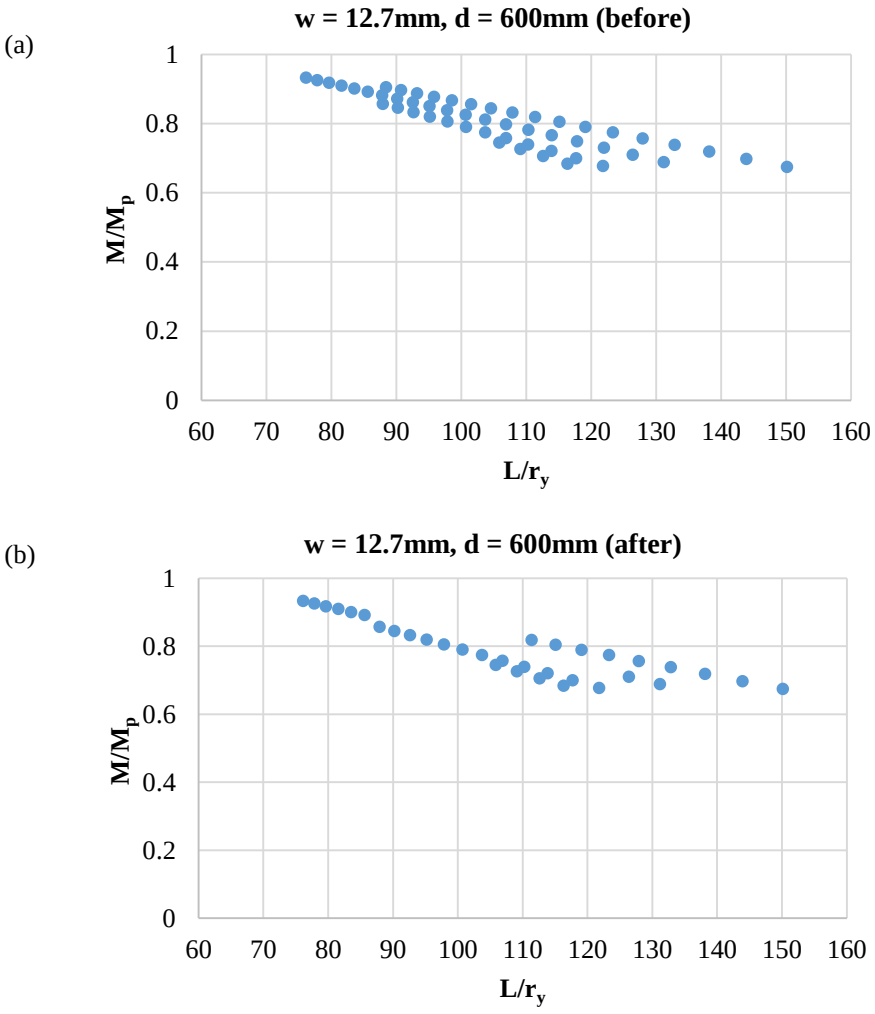

Figure 8: Possible test girders (a) before and (b) after residual stress sensitivity elimination

4.4 Test girder matrix

Of the 109 available sections, nine cross-section configurations are chosen and a total of 11 girders will be tested, as shown in Table 1. A five-part approach is used in the final selection process.

Table 1: Test girder matrix

No.	Serial No.[1]	Total Qty	w[2] (mm)	d (mm)	b (mm)	t[3] (mm)	d/b
SP1	G6-470-32-2-p	1	12.7	600	470	31.75	1.28
SP2	G6-430-32-1-f G6-430-32-1-p	2	12.7	600	430	31.75	1.40
SP3	G6-300-32-1-p	1	12.7	600	300	31.75	2.00
SP4	G8-430-25-2-p	1	12.7	800	430	25.4	1.86
SP5	G8-390-32-2-p	1	12.7	800	390	31.75	2.05
SP6	G8-390-25-2-p	1	12.7	800	390	25.4	2.05
SP7	G9-360-32-3-f G9-360-32-3-p	2	9.525	900	360	31.75	2.50
SP8	G9-360-25-3-f	1	9.525	900	360	25.4	2.50
SP9	G9-430-25-3-f	1	9.525	900	430	25.4	2.09

1. Serial number name convention is 'G' followed by: first digit of section depth – flange width – flange thickness – class – cutting method ('p' for plasma, 'f' for flame)
2. 9.525 mm and 12.7 mm web thicknesses correspond to 0.375 in and 0.5 in, respectively
3. 25.4 mm and 31.75 mm flange thicknesses correspond to 1 in and 1.25 in, respectively

4.4.1 Allowance for comparison of b and t

As flange width and thickness were identified as the critical cross-section dimensions, chosen test girders should allow the effect of b and t on LTB to be determined. For example, SP4 can be used as a flange width comparison for SP6 as all other cross-section dimensions are the same.

4.4.2 Aspect ratio

Defined as d/b, the aspect ratio indicates the stockiness or slenderness of the cross-section. Following Greiner and Kaim's (2001) distinction, "stocky" sections are considered to have $d/b \leq 2$ and "slender" sections have $d/b > 2$. The chosen girders should contain a range of stocky and slender sections to consider that the moment of inertia about the weak axis relative to that of the strong axis could have an effect on LTB.

4.4.3 Range of inelastic behaviour

To capture the complete spectrum of inelastic behaviour, the selected girders should cover a range of M/M_p or M/M_y and L/r_y, as shown in Fig. 9.

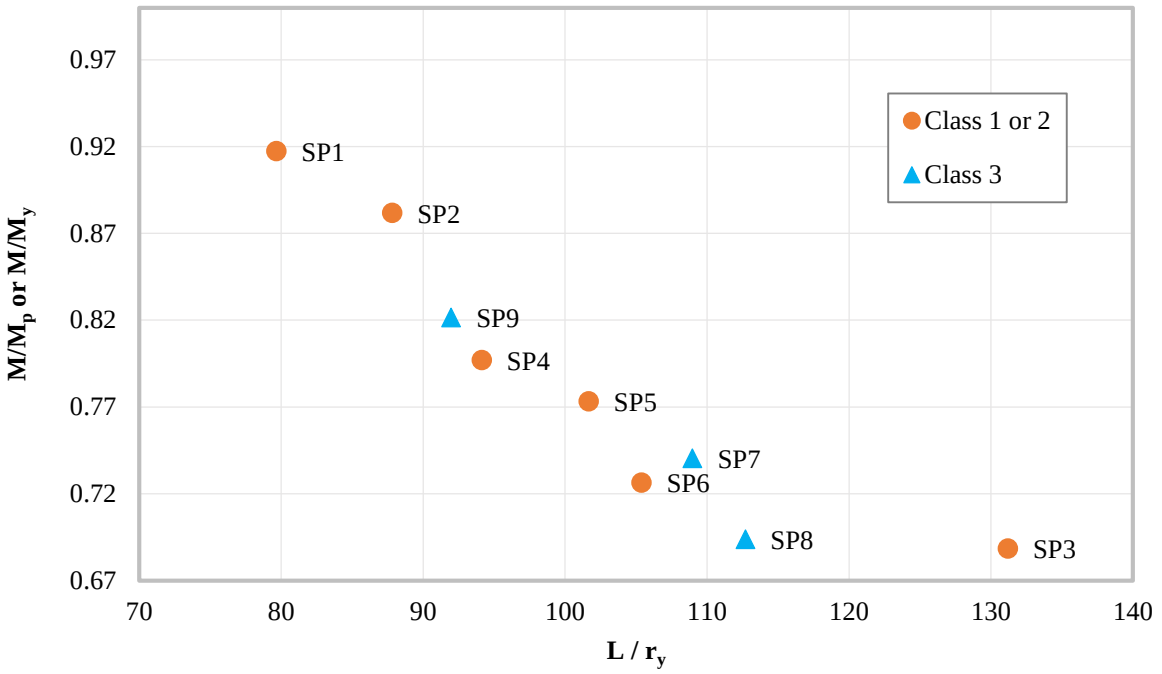

Figure 9: LTB resistance as a function of slenderness ratio for selected test specimens

4.4.4 Cutting method

The cutting method of the individual plates has been shown to have a large effect on residual stress (Ballio and Mazzolani 2013). To examine the resulting effect on LTB capacity, SP2 and SP7 are fabricated using two cutting methods: 1) flame-cutting; and 2) plasma-cutting. As no other properties change, the effect of cutting method is isolated for the two selected specimens.

4.4.5 Class of the section

For applicability to industry uses, the test matrix includes class 3 sections; this is because welded wide-flange girders that are commonly used in bridge construction comply with limits prescribed for class 3 sections. In addition to section class, girders are also chosen to include a range of flange class and web class, as shown in Fig. 10. In S16, LTB is separated into two categories: 1) at least class 2; and 2) class 3 sections. In reality, the flange and web of a member may fall into different categories, which could influence LTB resistance. Furthermore, the degree to which the flange and web falls into each category—i.e., firmly class 1 or at the cusp of class 1 and 2—could also create nuances in LTB strength and thus is important to consider.

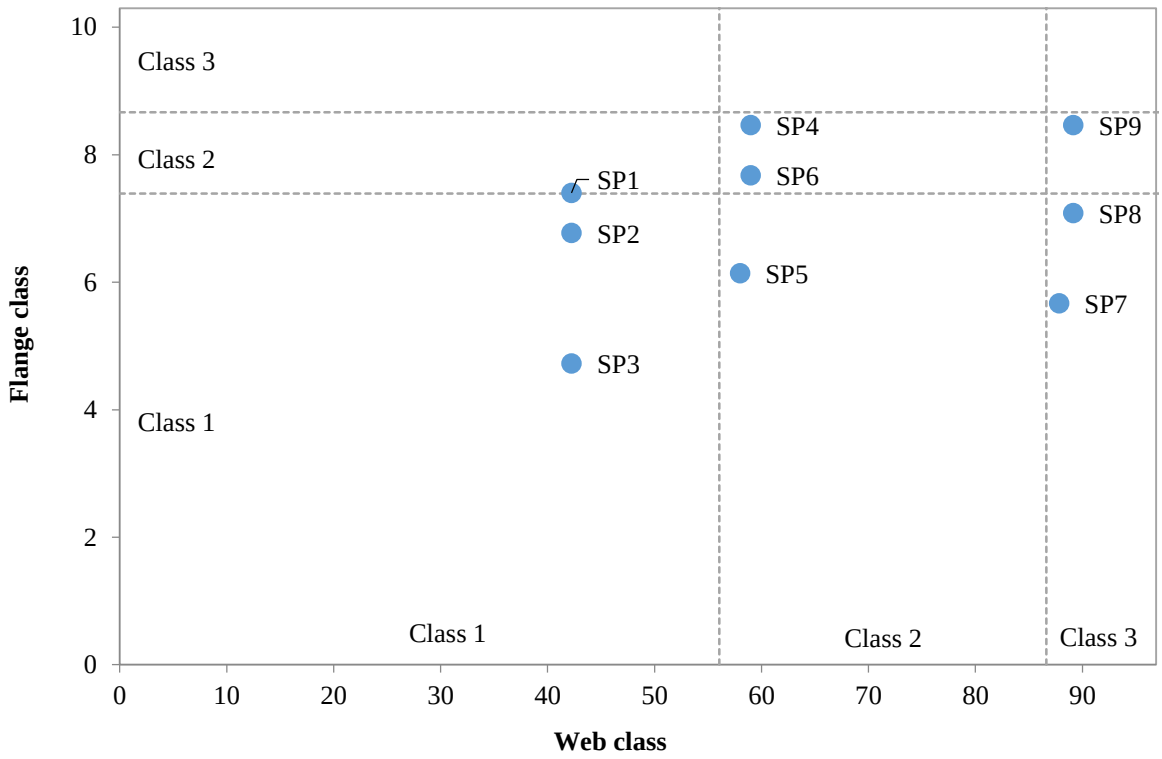

Figure 10: Flange and web classes of the selected test specimens

5. Conclusions

In recent years, the adequacy of the CSA S16 design provisions to predict lateral–torsional buckling has been questioned in literature. While numerical studies have indicated the design curve may be unconservative for welded sections in the inelastic lateral–torsional buckling range, there is a lack of experimental data to validate the numerical studies performed in the past and verify the design equations prescribed by S16. In response to this need, an experimental test program has been developed to evaluate the inelastic lateral–torsional buckling resistance of welded wide-flange girders; 11 test specimens of nine test girder cross-sections are proposed. Girders are 9.75m (32 ft) in length and loaded by eight concentrated loads. To allow for the out-of-plane deformation due to lateral–torsional buckling, a unique loading apparatus called the gravity load simulator is used to apply load through the top flange of the girder. This mechanism will maintain close-to-vertical load application even as the test girder sways and buckles out-of-plane. Each apparatus will apply a maximum load of 360 kN, with 20 kN of reserve capacity, and will remain elastic during the duration of testing. In designing the test girders, constraints of local buckling, lab capacity, shear strength, and inelastic lateral–torsional buckling reduced the 4,000 considered girders to 143. A stress-based analysis used to anticipate the effect of residual stresses further reduced the available sections to 109. Finally, a five-part criterion that considers the ability to compare b and t, aspect ratio, range of inelastic behaviour, plate cutting method, and section class is used to make the final test girder selection.

6. Future work

The main objective of the current stage of research is preparation for physical testing. Gravity load simulators have been designed and are in fabrication. Test girder drawings have been submitted and await fabrication. The remainder of the complex test set-up involves design of the collar and ancillary rod for loading. Occurring in tandem is the finalization of the components to allow sufficient degrees of freedom at the supports and load points.

Acknowledgments

The authors gratefully acknowledge Supreme Group for their contribution to this project, particularly Amir Jamshidi for his insight into test girder design; the financial assistance of NSERC; and the University of Alberta Steel Centre for challenging traditional boundaries of knowledge and research.

References

Baker, K.A., and Kennedy, D.J.L. 1984. "Resistance Factors for Laterally Unsupported Steel Beams and Biaxially Loaded Steel Beam Columns." *Canadian Journal of Civil Engineering*, 11 (4): 1008–19.

Ballio, G. and Mazzolani, F. 1983. *Theory and Design of Steel Strucutres.* New York: Chapman and Hall.

CSA. 2014. *CAN/CSA S16-14*.

CSI. 2015. "SAP2000 v14."

Dibley, J.E. 1969. "Lateral Torsional Buckling of I-Sections in Grade 55 Steel." *Proceedings of the Institution of Civil Engineers* 43 (4). ICE Publishing: 599–627.

Driver, R.G., Kulak, G.L., Elwi, A.E., and Kennedy, D.J.L. 1997. "Seismic Behaviour of Steel Plate Shear Walls." Structural Engineering Report 215. *Department of Civil and Environmental Engineering*, University of Alberta, Edmonton, AB.

Dux, P.F., and Kitipornchai, S. 1981. "Inelastic Beam Buckling Experiments." Research Report No. CE24. *Department of Civil Engineering*, University of Queensland, St. Lucia, QLD.

Fukumoto, Y. 1976. "Lateral Buckling of Welded Beams and Girders in HT 80 Steel." *IABSE Congress Report*, 403–8.

Fukumoto, Y., Fujiwara, M., and Watanabe, N. 1971. "Inelastic Lateral Buckling Tests on Welded Beams and Girders." *Japanese Society of Civil Engineers*, 39–51.

Fukumoto, Y., and Itoh, Y. 1981. "Statistical Study of Experiments on Welded Beams." *ASCE Journal of Structural Division*, 107 (1): 89–103.

Fukumoto, Y., Itoh, Y., and Kubo, M. 1980. "Strength Variation of Laterally Unsupported Beams." *ASCE Journal of Structural Division*, 106 (ST1): 165–81.

Fukumoto, Y., and Kubo, M. 1977. "An Experimental Review of Lateral Buckling of Beams and Girders." *International Colloquium on Stability of Structures Under Static and Dynamic Loads*, 541–62. ASCE.

Galambos, T.V. 1998. *Guide to Stability Design Criteria for Metal Structures*. 5thed. New York: John Wiley & Sons, Inc.

Greiner, R., and Kaim, P. 2001. "Comparison of LT-Buckling Design Curves with Test Results." *European Convention for Constructional Steelwork*, ECCS TC 8 Report 23. Brussels, Belgium.

Greiner, R., Salzgeber, G., and Ofner, R. 2001. "New Lateral Torsional Buckling Curves κLT - Numerical Simulations and Design Formulae." *European Convention for Constructional Steelwork*, ECCS Report 30. Brussels, Belgium.

Kabir, M.I., and Bhowmick, A.K. 2016. "Lateral Torsional Buckling of Welded Wide Flange Beams." (Master Dissertation). *Department of Building, Civil and Environmental Engineering*, Concordia University, Montreal, QB.

Kim, Y.D. 2010. "Behavior and Design of Metal Building Frames Using General Prismatic and Web-Tapered Steel I-Section Members." (Doctoral Dissertation). *School of Civil and Environmental Engineering*, Georgia Institute of Technology, Atlanta, GA.

MacPhedran, I., and Grondin, G.Y. 2011. "A Simple Steel Beam Design Curve." *Canadian Journal of Civil Engineering*, 38 (2): 141–53.

Mathworks. 2017. "MATLAB R2017a."

Subramanian, L., and White, D.W. 2017. "Resolving the Disconnects between Lateral Torsional Buckling Experimental Tests, Test Simulations and Design Strength Equations." *Journal of Constructional Steel Research*, 128: 321–334.

Timoshenko, S.P., and Gere, J.M. 1961. *Theory of Elastic Stability*. 2nd ed. New York: McGraw-Hill.

Wong-Chung, A. D., and Kitipornchai, S. 1987. "Partially Braced Inelastic Beam Buckling Experiments." *Journal of Constructional Steel Research*, 7 (3): 189–211.

Yarimci, E., Yura, J.A., and Lu, L.W. 1966. "Techniques for Testing Structures Permitted to Sway." Fritz Engineering Laboratory Report No. 273.40. *Department of Civil Engineering*, Lehigh University, Bethlehem, PA.